

Vascularized Dermopapilla 3D scaffold free Spheroids: an advanced micro-physiological system for hair growth research

Elisa Caviola¹, Francesca Rescigno¹, Robin Gradin² and Marisa Meloni^{1*}

¹ VitroScreen Srl, Italy; ² SenzaGen AB, Sweden.

* Corresponding Author: Marisa Meloni, VitroScreen Srl, via Mosè Bianchi 103, 0039-02-89077608, marisa.meloni@vitroscreen.com

Abstract

Background: Based on previously developed DermoPapilla (DP) model, a Vascularized DermoPapilla (VASC-DP) spheroid was developed by co-culturing primary human hair DermoPapilla cells (HHDPC) and microvascular endothelial primary cells (HMVEC). Their -omics signatures were established according to the dynamic evolution in micro-physiological systems (MPS).

Methods: The two models were cultivated up to 10 days (intermediate readout at day 5). The establishment of the co-culture and the formation of micro-vessels (CD31) and dermal ECM network (FN1) were evaluated by immunofluorescence. An -omic approach based Nanostring nCounter® technology was applied to investigate gene transcriptional signature and its evolution, focused on WNT pathway. Differentially expressed genes were identified and significantly modified gene sets were examined using GO enrichment analysis.

Results

Within the WNT pathway, the following gene clusters were identified as the most interesting to figure out model performances: matrix (ECM) structural protein and enzymes, proliferation markers (cyclins) and transcription factors related to hair follicle. Regarding a subset of genes involved in hair follicle growth, differences in expression were measured in time showing upregulation of IGFs, WNT5s and downregulation of DKK1 (WNT Inhibitor), that correlates with DermoPapilla growth. In VASC-DP, protein localization highlighted the presence of endothelial foci and vascular network integrated to DermoPapilla.

Conclusion: The 3D microenvironment, in presence of micro-vessels, provided the guidance for cells polarization and spheroids multi-compartmentalization resulting in a miniaturized functional organ with unique potential advantages, compared to other test systems in R&D studies on hair growth.

Keywords: 3D scaffold-free spheroids; vessels; hair follicle cycle; omics, MPS

Introduction.

The hair follicle (HF) is a self-renewing “mini-organ” acting as a biological clock which undergoes to continuous cycles of growth (anagen), regression (catagen) and quiescence state (telogen): these phases have a defined, perpetual unidirectional and highly regulated scheme in which a complex and fine-tuned interaction of signals induces deep metabolic and morphological changes. The human hair follicle remains less known than the murine counterpart, from which it differs for many morphological and functional aspects, but its study and use remain limited by its scarce availability. In fact, aesthetic plastic surgery is the only ethic source of human hair follicle but new, less invasive, techniques make the removal of the scalp, from which the follicles are extracted, unnecessary.

For all these reasons, countless efforts are made to create *in vitro* HF reconstructed models able to mimic its morphological and functional complexity. An ever-increasing complexity of *in vitro* models for research and screening is required to ensure the biological relevance and to mirror the *in vivo* situation. Tridimensional models are considered a golden standard since the bi-dimensional setting greatly limits the cell-to-cell contact, influencing the cell behavior and does not allow the production of the physiological extra cellular matrix (ECM) [1,2]. When the *in vitro* model is developed in a 3D environment, such as in a spheroid, the spatial 3D disposition, greatly modifies the contact cell-to-cell and cell-to-matrix ratio and it allows to better mirror the HF physiology. Furthermore, the increased cell-to-cell interaction affects a range of cellular functions [3], such as cell proliferation, differentiation, morphology, gene and protein expression, and cellular responses to external stimuli. All together these properties give to 3D spheroids a higher biological relevance and unique potential applications.

A study of Higgins et al. [4], focused on hair follicle DermoPapilla, demonstrated that the extraction of DermoPapilla fibroblasts and their cultivation in 2D systems alters their transcriptional profile but a partial restoring of gene expression can be achieved once the cells have been cultured in 3D. In our Laboratory we developed a hair follicle DermoPapilla scaffold-free spheroid model (Patent N. 102017000128725) composed by DermoPapilla

fibroblasts which can be cultured up to 14 days, presenting a transcriptional profile closer to *in vivo* DermoPapilla compared to bi-dimensional culture. Dermopapilla model is based on primary human cells and it mirrors phenotypic characteristics of the donor allowing a customizable selection specific parameter such as age and sex. The absence of exogenous scaffold, then, promotes the development of high morphological precision reflecting the native architecture of tissue and cells polarization. The culture conditions are optimized to guarantee a lifecycle up to 3 weeks during which the models show a dynamic evolution in its own micro-environment and functions as a miniaturized organ, mirroring the rhythm of the defined HF cycles.

Blood vessels, especially capillaries, surround hair follicles, are normally embedded within the dermal sheath and penetrating inside hair bulb surrounding DermoPapilla. The primary role of the blood vasculature in follicles is to deliver a constant supply of nutrients and other metabolites sufficient to match the metabolic requirements of metabolically active part of hair bulb, and therefore the size of the hair being produced. While there are limited literature findings in this area, there is evidence from mouse follicles that vascularity is increased around follicles during anagen [5]. The importance of vascularization in hair follicle growth can be deduced considering that a reference molecule of hair follicle stimulator (i.e. minoxidil) increases vascular blood flow and exerts a regulatory action on vascular network stimulating endothelial cells via VEGF increase [6].

Aim of this research project was to compare the existing HF model with the features of a co-culture model of DP fibroblasts with Human Microvascular Endothelial Cells (HMVEC). The -Omic precision signatures of the 2 models allowed deep transcriptomic investigations on the new vascularized DermoPapilla model, focused on WNT pathways due to its pivotal role in hair follicle biology and cycling coupled with specific proteins expression and spatial localization.

Materials and Methods.

Cells

Human Hair Follicle DermoPapilla cells (HFDPC) from a 51 y.o. female (Tebu-bio, France) were cultured in ready to use HFDPC Growth Medium (Tebu-bio, France) and Neo-der

Human Microvascular Endothelial Cells form pool of donors (HMVEC) (Lonza, Italy) were cultured in EGM™-2MV Basal Medium (CC-3156, Lonza, Italy).

VitroScreen ORA™ 3D scaffold- free spheroids production

At passage 5, HFDPC cells were detached by 0,05% Trypsin/EDTA solution (Lonza, Italy). Cells were counted and seeded to obtain 3D scaffold-free spheroids of 10000 cells each. Briefly, the method employed for spheroids generation was the Hanging Drop Technology by using specific culture plates (GravityPLUS and GravityTRAP plate, In Sphero, Zurich, Switzerland) allowing the development of scaffold-free spheroids using the gravity-mediated self-assembly strategy, avoiding the use of scaffolds or exogenous support.

For the vascularized model, after 40h from HFDPC seeding, HMVEC at passage 6 were detached by 0,05% Trypsin/EDTA solution (Lonza, Italy) and seeded in plates containing the spheroids. The amount of HMVEC cells was approx. 2000 cells per spheroids (HFDPC: HMVEC 4.5:1 in ratio). Standard DermoPapilla (DP) and vascularized (VASC-DP) spheroids were left on aggregation plates for total 4 days then they were transferred in culture plates and cultivated for 3, 5 and 10 days. During this period the co-culture was maintained using a medium composed by HFDPC Growth Medium and in EGM™-2MV Basal Medium in a 1:3 ratio.

Viability by ATP release

The kit CellTiter Glo (G7570, Promega) Luminescent Cell Viability Assay is used for Adenosine -5- triphosphate (ATP) quantification. The assay procedures involves adding the single reagent directly to spheroids (n=6) . The cell lysis and the generation of a luminescent signal is proportional to the amount of ATP present. The system can detect a stable luminescent signal, 20 minutes after adding reagent and mixing. To obtain a quantitative ATP evaluation, a standard curve with the following ATP concentrations is used: 0 nM, 100 nM, 500 nM, 1000 nM, 10000 nM.

Total RNA extraction by RNeasy MicroKit

RNeasy MicroKit by Qiagen (cat.74004) was used to extract the total RNA form spheroids with the advantage of a low volume of elution in order to enrich RNA concentration. Total

RNA was extracted by 3 pools of 25 spheroids each following the manufacturer's instructions. RNA was eluted in RNase free water and stored at -80°C until use. 2 μ l of RNA were used to perform QC by 2100 Bioanalyzer (Agilent) on Agilent RNA 6000 Nano Chip with Agilent RNA 6000 Ladder and Reagent. The method is based on capillary gel electrophoresis. For each sample, total RNA content and RNA Integrity Number (RIN) was calculated. All RNA samples were verified against the RNA acceptance criteria.

Gene expression analysis using Nanostring nCounter System

The NanoString platform quantifies genes that have been specifically targeted in an analysis. The Vantage 3D™ RNA Wnt Pathways Panel CodeSet (VRXC-Wnt1-12, Nanostring Technologies, Seattle, WA) includes probes for 192 genes, 180 of which are related to Wnt signaling. The remaining 12 genes are termed housekeeping genes and were used for purposes such as normalization and quality assessment.

A total of 100 ng of RNA was used as sample input in a hybridization assay with the WNT Pathway CodeSet. Each hybridized sample was prepared on cartridge using nCounter MAX Prep Station and individual transcripts of the endpoint specific biomarker signature were quantified using nCounter MAX Digital Analyzer (NanoString Technologies, Seattle, WA). The output data, relative to the single transcript counting for each analyzed genes, were verified against the Acceptance criteria before proceeding to bio-statistical analysis.

Biostatistical analysis of transcriptomic analysis

The gene expression analyses were performed in R 4.1.1 [7]. The quality of individual samples was assessed by considering the NanoString quality parameters, including binding density, imaging quality, linearity of positive spike-in probes, limit of detection, and the number of acquired counts for the positive spike-in probes. In addition, the data quality was further evaluated with techniques such as principal component analysis (PCA) and relative log error plots [8].

Sample-specific thresholds for limit of detection were calculated using the negative spike-in probes present in the NanoString codeset. The threshold was defined as the probes' mean expression values plus two standard deviations ($\mu + 2\sigma$). Genes that were consistently expressed below the limit of detection were considered undetectable in the experiment and

were excluded from subsequent analyses. Genes were categorized into five different categories based on the magnitude of their expression levels across the samples. The categories were defined as not expressed (below 21 counts), low (21-100 counts), moderate (100-500 counts), high (500-2000 counts), and very high (above 2000 counts).

The differential expression analysis was performed using edgeR 3.34.1 [9,10]. P-values were adjusted for multiple hypothesis testing using the Benjamini & Hochberg procedure [11] (false discovery rate [FDR]), and genes with FDRs below 0.05 was considered significantly differentially expressed. Gene ontology (GO) enrichment analysis was performed using Fisher's exact test, using the measured genes as background list and genes with a P-value from the differential expression analysis below 0.05 as input (for assessment of overrepresentation), analyzing up- and downregulated genes separately. PCA was performed on standardized (i.e., centered and scaled, $\mu=0$ and $\sigma=1$) expression levels for expressed genes.

Whole mount spheroids Immunolabelling

DP and VASC_DP spheroids after 5 and 10 days of culture were collected for immunolabelling in whole mount. Samples were washed in PBS 1X and fixed in formalin buffered solution 10% (Merck, Dramstadt, Germany) for 1h at RT. After tissue fixation, samples were prepared for histological clearing before incubation with primary antibody. Visikol Histo-M Starter Kit® (Visikol, Hampton, NJ, USA), was used as clearing reagent and samples were treated according to internal procedure: pooled samples ($n = 7$ spheroids/each pool) were de-hydrated and re-hydrated with cycles of 15 min each by incubations with increasing concentrations of ET-OH solutions (from 50% to 100%). After permeabilization with PBS-Triton solution 0.2% and Visikol Histo® Permeabilization Buffer, the blocking of a-specific sites was performed by incubation with Visikol Histo® Blocking Solution. Samples were incubated with CD 31 mouse monoclonal primary antibody (Abcam, cat. ab9498) and fibronectin rabbit polyclonal primary antibody diluted (Abcam, cat. ab2413) in Visikol Histo® Antibody Buffer overnight at 4°C. Alexa 488 goat anti-mouse (Life Technologies, 1:600) and 555 donkey anti-rabbit (Life Technologies, 1:800) were used as secondary antibody while nuclei were stained with DAPI (Merck, 1:2500). Stained Vascularized-DP spheroids were cleared with Visikol Histo®-M overnight at 4°C. The

acquisitions were performed by Leica THUNDER DMi8 3D Cell Imager and Z-stacks movies were acquired with a Leica sCMOS Camera and post-processed by LASX 3.0.1 software. Z-stacks were acquired to observe the whole volumes of 3D spheroids and expression signals were optimized by Thunder Computational Clearing algorithm. Three more informative frames were extrapolated from the Z-stack movies, for each sample.

Results

Transcriptome analysis by NanoString

The viability of the spheroids was assessed both in DP and VASC-DP at two time points by measuring ATP on spheroid lysates and no significant modifications were recorded (data not shown).

Transcriptome analyses were performed starting from the counting of single transcript of 180 genes present in the Nanostring Vantage 3D-WNT-Pathway CodeSet.

The observed gene expression levels were separated into 5 discrete categories based on their expression levels (from below detection limit to very high). Although the actual thresholds and the count categories are in nature arbitrary this distinction is informative of the magnitude of counts. The obtained results showed a normal distribution of WNT pathway genes among expression level categories indicating the relevance of the selected pathway for hair follicle model description.

Among all genes, the attention was focused on the genes with expression levels high and very high to assess the main transcriptional features. The most expressed genes comprise structural extra cellular matrix (ECM) protein (e.g. FN1 and collagens), enzymes for ECM homeostasis (MMPs and TIMP, proteases), proliferation markers (cyclins) and transcription factors related to hair follicle. Moreover, among WNT-related genes, a subset was selected based on literature about the key-regulators of hair follicle cycle to assess the hair follicle features in the produced models. This subset was composed by WNTs, anagen related FGF7 and IGFI, proliferation-related genes and DKKs as anagen inhibitors. Furthermore, in this case the gene distribution in expression level categories was homogeneous indicating a balanced transcriptional activity with high expression of fundamental hair follicle markers as WNT5A/B and VEGF.

Biostatistical methods for the reduction of dimensionality were applied to capture difference in DP model versus new VASC model. PCA analysis showed that the highest variability was present between the two models indicating an actual contribution of endothelial compartment in transcriptional activity of spheroids. A secondary component of variability was due to timing: in fact, as expected, changes in transcriptional profiles were due to the times of culture, indicating the evolution of the models during the culture (Fig.1).

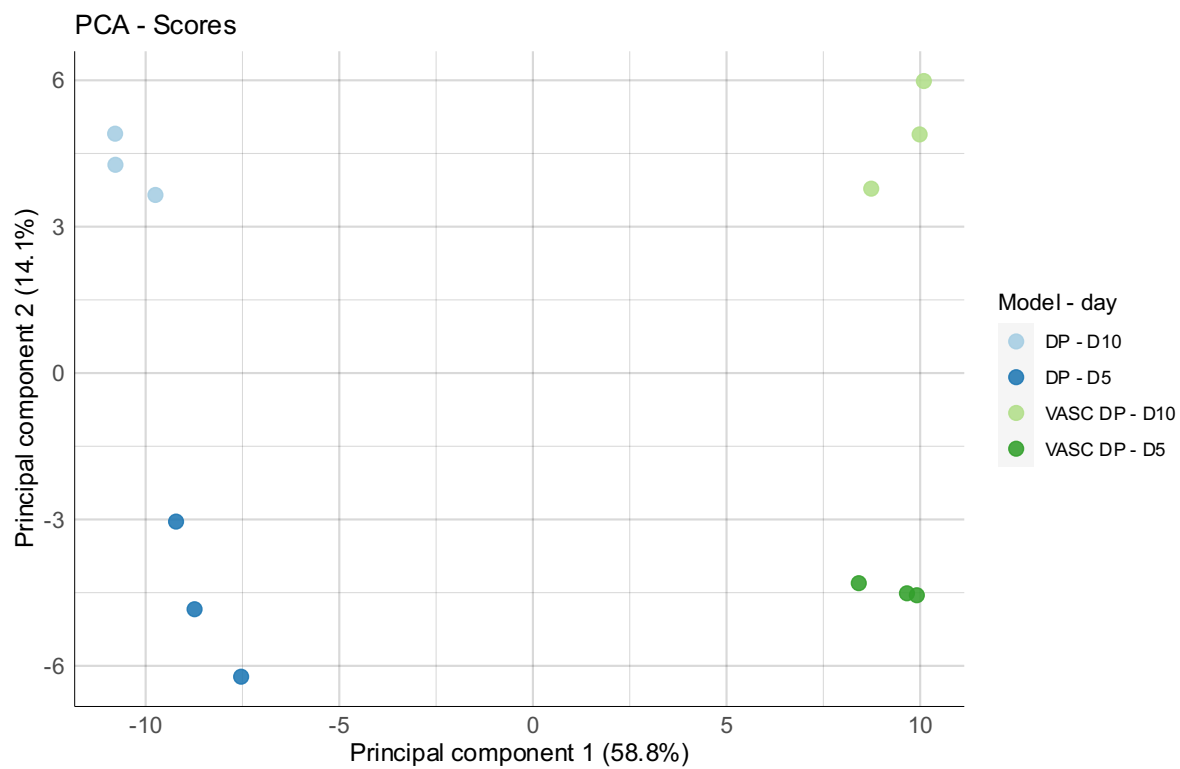


Fig.1 Principal component analysis (PCA) on normalized expression values for DP and DP-VASC models at day 5 and day 10 of culture

Differential gene expression (DGE) was performed in both models comparing the day 5 versus day 10 and the specific transcriptional signatures are reported as heat-map (Fig. 2).

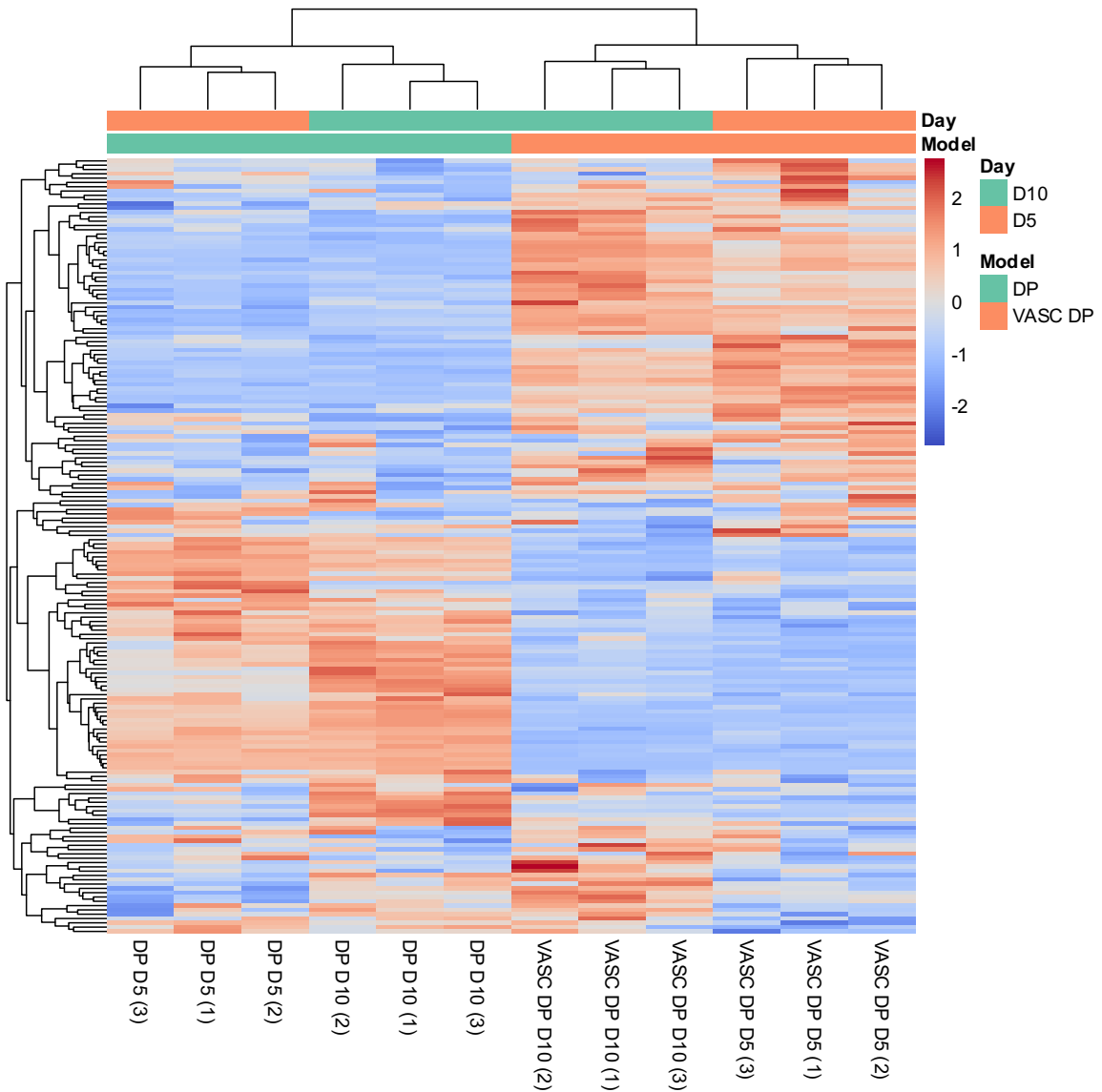


Fig.2 Differential gene expression (DGE) analysis heatmap of normalized expression values for DP and DP-VASC models at day 5 and day 10 of culture

As reported by DGE heatmap, according to PCA, the DP and VASC-DP models present very different transcriptional profiles regarding WNT pathway. For each model, different gene expression patterns have been underlined and a further discrimination between the 2 models response has been observed during the dynamic evolution of the culture (day 5 and day 10).

Considering the p value threshold of 0.05, the statistically significant genes with different expression were identified and divided in upregulated and downregulated groups. Gene Ontology enrichment (GO) was performed on each group in order to identify expression patterns and pathways and to describe the possible evolution of transcriptional signature in time. Among GO genes annotated in skin upregulation involved positive regulators of proliferation, cell surface receptor for signaling, negative regulators of apoptosis and tissue development genes; on the contrary, the negative regulators of cellular process resulted downregulated, that correlates with DP growth.

Immunofluorescence

VASC-DP spheroids were stained by whole mount immunofluorescence to analyses the composition of DermoPapilla ECM (by FN1, fibronectin expression) and microvascular network (by CD31 expression) preserving the 3D model structure and the natural architecture of each compartment. The most representative timepoint was day 5 in which a homogeneous distribution of FN1 was present, indicating a mature ECM network, and an early vascular network were endothelial cells started to polarize inside the endogenous ECM of DermoPapilla stroma. Thin vessels-like structures are visible inside the stromal core between different optical planes. Foci of early junctions are randomly localized as points of greater signal intensity of CD31 indicating spouting points of neo-branches formation.

Discussion.

Joining advanced techniques to produce tridimensional cellular models as MPS and the cutting-edge -omics technology for model characterization, we developed a new hair follicle as 3D spheroid combining DermoPapilla core with endothelial compartment an characterized its transcriptional profile focusing on WNT pathway and its role in hair follicle cycle. Different levels of biostatistics were used considering, as first approach, all the biological samples of the two models in their globality to demonstrate the relevance of the chosen gene panel and then carrying out direct comparisons between conditions to characterize the specific model models.

In canonical Wnt/β-catenin signaling, the secreted Wnt proteins bind with the Frizzled receptor and a co-receptor of the low-density lipoprotein-related protein (LRP), thereby inactivating glycogen synthase kinase-3 (GSK-3), which is an enzyme responsible for

phosphorylation and ubiquitination-mediated degradation of β -catenin. In this way β -catenin is stabilized, accumulates in cytoplasm and binds with T-cell factor (TCF)/lymphoid enhancer factor (LEF) translocating in the nucleolus and causing the transcriptional activation of genes involved in the regulation of anagen progression [12, 13]. Multiple evidence suggest that various Wnts promote hair cycling and regeneration via the activation of β -catenin signaling. Among the Wnt family Wnts 2, 7b, 10a, and 10b (called secondary Wnts) participate in HF development and are related to hair follicle cyclic regeneration [14,15]. The presence of Wnt3a was shown to activate β -catenin and increased hair growth in nude mice receiving skin reconstitution composed of DP and keratinocytes [16]. On the contrary, the inhibition of Wnt pathway cause the loss of regenerative potential of hair follicle. In fact, the overexpression of Dickkopf 1 (DKK1), a Wnt inhibitor, leads to an early and complete block in the development of skin appendages including all types of hair follicles, thus suggesting the essential roles of WNT proteins in follicle development [17]. Moreover, an increase of DKK1 immunostaining was found in lesional scalp biopsies taken from patients with androgenic alopecia and alopecia areata as compared to healthy control volunteers confirming the importance of Wnt pathway in hair follicle cycle [18]

The application of descriptive biostatistical analysis reduction of dimensionality of data [19] showed that WNT pathway is relevant for both DP and VASC-DP model although their transcriptional signature resulted different due to endothelial cells contribution and the that transcriptional profile evolve during time in culture. A comparison between differentially expressed genes was performed using DGE analysis followed by application of enrichment analysis techniques as Gene Ontology (GO). GO enrichment analysis is commonly used for interpreting high throughput molecular data and generating hypotheses about underlying biological mechanisms [20]. This approach allowed to detect pathways within WNT cascade that were positively or negatively modulated during the time and to assess that, up to 10 days, in the VASC-DP model specific pathways related to vascularization as cell and tissue proliferation and modelling are modulated while in the DP model the pathways related to hair-follicle phases were better described. Morphological analysis of VASC-DP spheroids has confirmed the establishment of endothelial network of tubules and primordial vessels. Advanced biostatistical analyses were applied to better describe the transcriptional activity and asses a potential progression toward more regressive status (catagen-like) and to monitor

the evolution of vascular network and ECM matrix of DermoPapilla compartment. The data interpretation of these supplementary analyses is in progress.

Conclusion.

In the present study, state-of-the-art technologies were combined to create an advanced and unique micro physiological system: from one side advanced tissue engineering generated an *in vitro* vascularized DermoPapilla spheroid model and from the other side digital barcoding transcriptome analysis was applied to its characterization extrapolating the precise omics signature. VASC DP was developed within the ORATM platform that represents an evolute system to generate 3D scaffold free spheroids, precisely designed in their natural microscale 3D architecture on 96 well plates. Each ORATM spheroid produces its own micro-environment and functions as a miniaturized organ with ECM deposition, organization and metabolism, letting the physiological mechanisms occur slowly, relying on cell-matrix interaction, mirroring phenotypic characteristic of the donor's cells. Indeed their most relevant characteristics is to better mimic *in vivo* physiology: the miniaturized scaffold-free spheroids are a functional biomimetic system to investigate complex biological processes and to monitor the dynamic evolution of single compartments. The quantitative analysis of -omics high content datasets for gene expression, performed by NanoStringTM, allowed to characterize the genetic signature of hair follicle models, starting from the WNT pathway, fundamental for the morphogenesis of the hair follicle.

The vascularized DermoPapilla model showed a different transcriptional profile from the standard DermoPapilla due to the contribution of endothelial cells. An evolution of the transcriptome up to 10 days of culture in both models was demonstrated, showing the different modulation of genes related to active phase of DP growth and proliferation as well tissue remodeling as hair growth cycle. Protein expression and spatial localization of key biomarkers was performed by a LED technology for quantitative non-destructive analysis on 3D whole mount live cells samples. The morpho-histological evaluation of vascularized model for the visualization of dermal papilla structure and endothelial network by using whole mount immunostaining and computational imaging, confirmed the formation of an vascular network which mimic the Dermal Papilla architecture present in *in vivo* hair bulb.

Acknowledgments. We thank Lisa Theorin and Per Alftren at SenzaGen SA for their excellent technical contribution to this work by performing NanoString analysis.

Conflict of Interest Statement. None

References.

1. Kim JB (2005) Three-dimensional tissue culture models in cancer biology. *Semin Cancer Biol* 2005; 15:365–377.
2. Khaitan D, Chandna S, Arya MB, Dwarakanath BS (2006) Establishment and characterization of multicellular spheroids from a human glioma cell line; Implications for tumor therapy. *J Transl Med* 4:1–13
3. Lin RZ, Chang HY (2008) Recent advances in three-dimensional multicellular spheroid culture for biomedical research. *Biotechnol J* 3:1172–1184
4. Higgins C, Chen JC, Cerise JE, Jahoda CA, Christiano AM (2013) Microenvironmental reprogramming by three-dimensional culture enables DermoPapilla cells to induce de novo human hair-follicle growth. *Proc Natl Acad Sci U S A*. 2013 Dec 3;110(49):19679-88.
5. Yano K, Brown LF, & Detmar M (2001) Control of hair growth and follicle size by VEGF-mediated angiogenesis. *The Journal of Clinical Investigation*, 107(4), 409–417
6. Messenger AG, Rundegren J (2004). Minoxidil: mechanisms of action on hair growth. , 150(2), 186–194
7. R Core Team (2021) R: A Language and Environment for Statistical Computing. Vienna, Austria. <https://www.R-project.org/>
8. Gandolfo LC, Speed TP (2018) RLE plots: Visualizing unwanted variation in high dimensional data. *PLoS ONE* 13(2): e0191629. <https://doi.org/10.1371/journal.pone.0191629>
9. Robinson MD, McCarthy DJ, Smyth GK (2009) edgeR: a Bioconductor package for differential expression analysis of digital gene expression data. *Bioinformatics*, 26(1), 139–140. doi:10.1093/bioinformatics/btp616
10. McCarthy DJ, Chen Y, Smyth GK (2012). Differential expression analysis of multifactor RNA-Seq experiments with respect to biological variation. *Nucleic Acids Res*. 2012

May;40(10):4288-97. doi: 10.1093/nar/gks042. Epub 2012 Jan 28. PMID: 22287627; PMCID: PMC3378882.

11. Benjamini Y, Hochberg Y (1995) Controlling the False Discovery Rate: A Practical and Powerful Approach to Multiple Testing. *Journal of the Royal Statistical Society: Series B (Methodological)*, 57(1), 289–300. doi:10.1111/j.2517-6161.1995.tb02031.x
12. Bejsovec A, (2000) Wnt signaling: An embarrassment of receptors. *Curr. Biol.* 10, R919–R922.
13. Wodarz A, Nusse R (1998) Mechanisms of Wnt signaling in development. *Annu. Rev. Cell Dev. Biol.* 14, 59–88.
14. Andl T, Reddy ST, Gaddapara T, Millar SE (2002) WNT signals are required for the initiation of hair follicle development. *Dev. Cell*, 2, 643–653.
15. Zhang Y, Tomann P, Andl, T, Gallant, NM, Huelsken J, Jerchow B, Birchmeier W, Paus, R, Piccolo S, Mikkola M.L. (2009) Reciprocal requirements for EDA/EDAR/NF-kappaB and Wnt/beta-catenin signaling pathways in hair follicle induction. *Dev. Cell* 17, 49–61
16. Xiong Y, Liu Y, Song Z, Hao F, Yang X (2014) Identification of Wnt/beta-catenin signaling pathway in DermoPapilla cells of human scalp hair follicles: TCF4 regulates the proliferation and secretory activity of DermoPapilla cell. *J. Dermatol.* 41, 84–91
17. Bafico A, Liu G, Yaniv A, Gazit A, Aaronson SA, (2001) Novel mechanism of Wnt signalling inhibition mediated by Dickkopf-1 interaction with LRP6/Arrow. *Nat. Cell Biol.* 2001, 3, 683–686.
18. Mahmoud EA, Elgarhy LH, Hasby EA, Mohammad L, (2019) Dickkopf-1 Expression in Androgenetic Alopecia and Alopecia Areata in Male Patients. *Am. J. Dermatopathol.* 41, 122–127.
19. Van Der Maaten L, Postma E, Van Den Herik J (2009). "Dimensionality Reduction: A Comparative Review". *J Mach Learn Res.* 10: 66–71.
20. Botstein D, Cherry, JM, Ashburner M, Ball CA., Blake JA, Butler HD, Allan P, Dolinski K, Dwight SS, Eppig JT, Harris MA, Hill DP, Issel-Tarver L, Kasarskis A, Lewis S, Matese JC, Richardson JE, Ringwald M, Rubin GM, Sherlock G (2000). Gene Ontology: tool for the unification of biology. *Nature Genetics*, 25(1), 25–29.